

# Thermal Analysis of Power Cables in Free Air: Evaluation and Improvement of the IEC Standard Ampacity Calculations

Ali Sedaghat, *Student Member, IEEE*, and Francisco de León, *Senior Member, IEEE*

**Abstract**—The thermal behavior of cables installed in free air depends upon physical parameters, such as surface emissivity, heat dissipation coefficients for radiation and natural convection, as well as induced heating from neighboring heat sources that depend on the configuration in which the cables are grouped. The IEC standard method for rating cables installed in free air considers all of these physical properties implicitly and only for particular conditions. In this paper, the IEC standard method for rating power cables installed in free air is evaluated against finite-element method simulations and laboratory experiments. A scientifically sound and accurate thermal-electric circuit for the calculation of the steady-state temperature of cables in air is derived from first thermodynamic principles. The model parameters are computed explicitly from the physical properties of the cable, cable grouping, and environment. Through numerous finite-element simulations, as well as laboratory experiments, the accuracy of the proposed method has been established.

**Index Terms**—Cable ampacity, cables installed in free air, cable thermal analysis.

## I. INTRODUCTION

CABLE THERMAL analysis in power systems is a very important component of the system design. The defining factor for cable ampacity is the maximum temperature attained by the conductor. Among the various installation methods, one of the most commonly used is to set cable in free air. The IEC Standard IEC-60287-2-1 [1], in Section 2.2.1, proposes an iterative method for the calculation of cable surface temperature above ambient temperature ( $\Delta\theta_s$ ). The thermal resistance external to a cable in free air, where the heat transfer between cable and supporting system is negligible and isolated from solar radiation, is given by

$$T_4 = \frac{1}{\pi D_e^* h (\Delta\theta_s)^{1/4}} \quad (1)$$

where

$$h = \frac{Z}{(D_e^*)^g} + E \quad (2)$$

Manuscript received August 21, 2013; revised November 11, 2013; accepted December 08, 2013. Date of publication January 17, 2014; date of current version September 19, 2014. Paper no. TPWRD-00953-2013.

The authors are with the Electrical and Computer Engineering Department, NYU Polytechnic School of Engineering, Brooklyn, NY 11201 USA (e-mail: Sedaghat@nyu.edu; fdeleon@poly.edu).

Color versions of one or more of the figures in this paper are available online at <http://ieeexplore.ieee.org>.

Digital Object Identifier 10.1109/TPWRD.2013.2296912

is the heat dissipation coefficient ( $\text{W}/\text{m}^2 (\text{K})^{5/4}$ ),  $D_e^*$  is the external diameter of cable (in meters);  $Z$ ,  $E$ , and  $g$  are constants which are given in [1] in tables.  $h$  is a function of cable surface and ambient temperature [2]. The cable surface temperature is factored in the external thermal resistance (1) and  $h$  reflects the all modes of heat transfer as well as mutual heating effects for fixed operating conditions [3]. The heat transfer for cables installed in free air occurs through radiation and natural convection. Each of these physics has its own heat dissipation coefficient given by [4]

$$h_{\text{rad}} = \varepsilon \sigma (T_s + T_{\text{amb}}) (T_s^2 + T_{\text{amb}}^2) \quad (3)$$

$$h_{\text{conv}} = \frac{Nu k_{\text{amb}}}{D_e^*} \quad (4)$$

where  $h_{\text{rad}}$  is the radiative heat-transfer dissipation coefficient,  $\varepsilon$  is emissivity of the cable surface,  $\sigma$  is Stefan–Boltzmann constant,  $T_s$  is the temperature of the cable surface,  $T_{\text{amb}}$  is the ambient temperature,  $h_{\text{conv}}$  is the convection heat dissipation coefficient,  $Nu$  is the Nusselt number, and  $k_{\text{amb}}$  is the thermal conductivity of air at ambient temperature. According to (2), the IEC considers a combined heat dissipation coefficient  $h$  for radiation and convection. From (3) and (4), it is obvious that both heat coefficients are functions of ambient and cable surface temperatures. Notice that  $Nu$  is a function of cable surface and ambient temperatures as well [4].

The scope of the IEC standard, which unfortunately is not given in the standard, seems to be for emissivity of 0.9, cable surface temperature around 80 °C, and ambient temperature around 30 °C [5]. Therefore, the IEC approach may be improved when the operating conditions are different from those used by the standard.

The calculation of cable temperature in IEC-60287-2-1 [1] is based on the work by Whitehead and Hutchings [6]. In 1969, Slaninka [7] proposed new formulas for heat coefficients for the most important installation cases to improve the Whitehead and Hutchings method. He considered the variation of  $h$  by including the cable surface temperature and the effect of surface emissivity. In 1994, Morgan [2] criticized the IEC method and produced more accurate constant coefficients ( $Z$ ,  $E$ ,  $g$ ) than those introduced in [1]. This was done by considering the effect of surface temperature rise and the calculation of  $h$  for single, two, and trefoil cables in air. Morgan in [8] proposed an equivalent external diameter for bundled cables based on the imaginary circle that circumscribes the bundle. In this paper, through numerous finite-element method (FEM) simulations, it is proven that Morgan's approximation is not very accurate.

In this paper, the validity of the IEC Standard for different installation methods for cables in air is analyzed. The effect of all critical parameters is investigated and a thermal-electrical circuit for the accurate steady-state rating for the most common installation configurations is proposed. The new model has been validated with many FEM simulations and laboratory experiments. Another contribution of the paper is the proposal of accurate equations for the calculation of the total heat dissipation coefficient for cables touching and separated for horizontal grouping. This is verified with FEM parametric studies, laboratory experiments, and analytical investigations.

## II. EVALUATION OF IEC STANDARD CALCULATION METHODS FOR CABLES INSTALLED IN FREE AIR

### A. Finite-Elements Model

Transient heat-transfer FEM simulations are performed until the steady state is reached as was done in [9]. All of the finite-element simulations of this paper were performed using the non-isothermal heat-flow module of COMSOL Multiphysics [10]. The steady-state engine of COMSOL does not seem capable of finding directly the final steady-state temperature of cables installed in free air for most of the cases. Therefore, it was necessary to perform long transient simulations to reach steady state. COMSOL solves the complete computational fluid dynamics (CFD) problem. For each simulation, a 2-D geometry and a time-dependent solver is used. Depending on the geometrical particularities of the model, the computer time can vary from a few hours and up to several days to simulate 6 to 12 hours of actual cable life (transient response to reach steady-state conditions) using a server that has 24 cores in its CPU, each core clocking at 3.33 GHz, and 192 GB of DDR3 RAM. In the Appendix, a link is provided to download the COMSOL files to reproduce the FEM simulations.

In all FEM simulations, cables have been placed in a box that properly represents the surrounding free air (see Fig. 1). Surrounding air is defined by a box composed of four boundaries, labeled 1, 2, 3, and 4. Boundaries 1 and 4 are thermal insulation. They are placed sufficiently far from the cables to prevent any influence in the results. Boundary 2 is an air inlet and its temperature is fixed at the ambient temperature. Boundary 3 is an outlet for airflow. In this way, still air surrounds the cables and natural convection and radiation can occur. The distances between the boundaries and the cable have been obtained by trial and error for all cable arrangements. It was ensured that the results of the FEM simulations are not affected in any way by the location of the boundaries.

Two different types of meshing are used. Inside the cable, fine meshing that is adequate for general physics is used. Outside the cable, where nonlinear phenomena occur, finer meshing that is adequate for fluid dynamics is used. Triangular meshing has been used inside and outside. Frequently, the triangles where circular shapes touch are of special concern during the meshing process. However, there were no problems with the aforementioned meshing setup. In this case, none of the triangles ever degenerates, thus no special meshing techniques were necessary. The variation of the *ac* resistance with temperature has been taken into account in the FEM simulations following the IEC

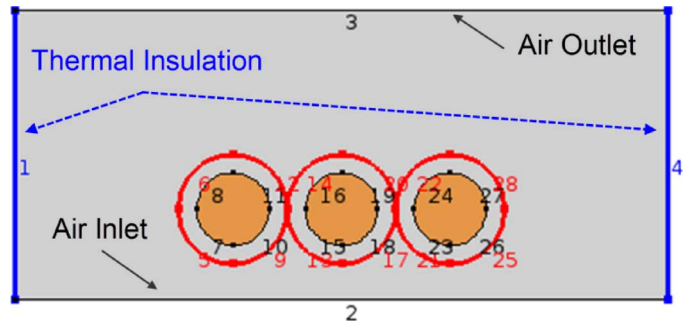


Fig. 1. Geometry of the FEM simulation as built in COMSOL for a group of horizontal touching cables.

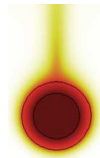


Fig. 2. Distribution of the steady temperature field for a single-core cable.

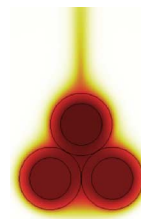


Fig. 3. Distribution of the steady temperature field for a trefoil formation (touching cables).

Standard 60287-1-1. The accuracy of FEM simulation has been established by comparing the results versus laboratory experiments in Section III.

### B. One Single-Core Cable

Without loss of generality, the simple single-core cable described in Fig. 18(a) (see the Appendix) is considered for the analysis since only the properties of the outer surface are needed. The final temperature attained by the hottest point in the cable is obtained from FEM for different resistive losses. Emissivity of cable surface is considered to be 1.0 (black body). Fig. 2 shows the temperature field in steady state. The results of a parametric study comparing the IEC method against FEM show that there is a good match between the two. The sole visible difference between FEM and IEC results is that the IEC temperature calculations show linear variation with respect to losses, while FEM shows a slightly nonlinear dependence (see the details in Fig. 10). Although the error in the IEC method for this case is negligible, incorrect modeling yields substantial errors for cable groupings as will be discussed.

### C. Trefoil Touching Formation

A widely used installation method for cables, especially in three-phase systems, is the trefoil touching formation. For the calculation of the steady-state temperature of this formation, the IEC [1] assumes that all cables have the same final temperature.

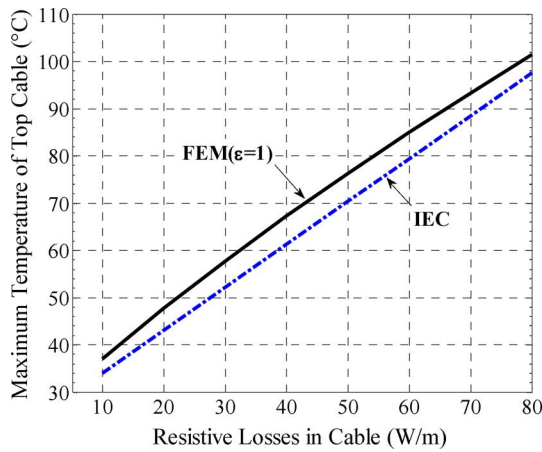


Fig. 4. Steady-state temperature for the conductor of the hottest cable (top cable) in the trefoil formation with 25°C ambient temperature. The cable construction is given in Fig. 18(a).

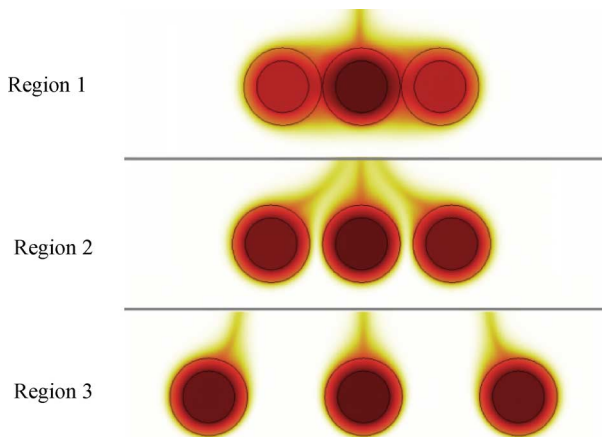


Fig. 5. Distribution of the steady temperature field for a group of horizontal cables, touching and not touching; regions 1, 2, and 3, respectively.

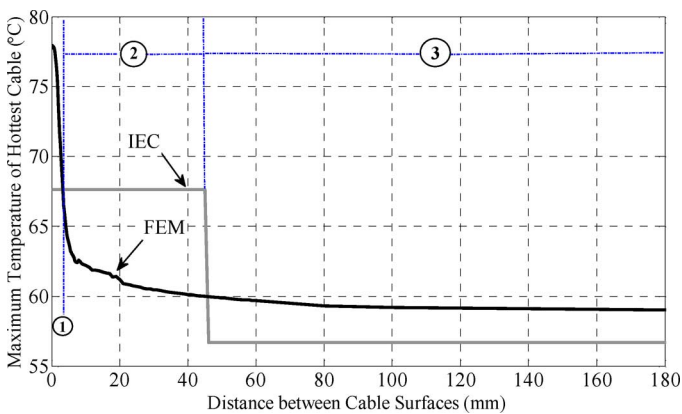


Fig. 6. Steady-state temperature for the conductor of the hottest (center) cable in the group at 25°C ambient temperature and 50-W/m power losses in each cable. The cable construction is given in Fig. 18(a).

The heat dissipation coefficient is computed with (2) by using the corresponding constant coefficients ( $Z$ ,  $E$ , and  $g$ ) for the trefoil formation. Three equally loaded cables are assembled in a trefoil formation as shown in Fig. 3. Transient FEM simulations are performed until the steady state is reached. The emissivity

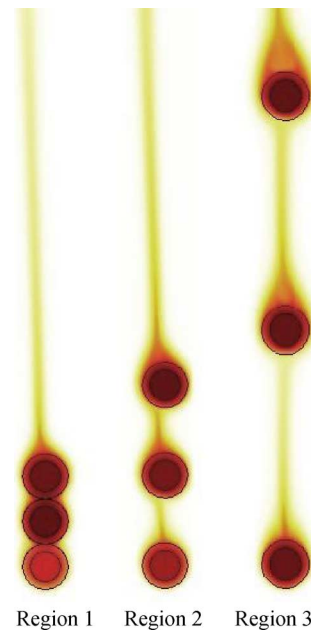


Fig. 7. Simulation of a group of vertical cables touching and not touching arrangements (Regions 1, 2, 3).

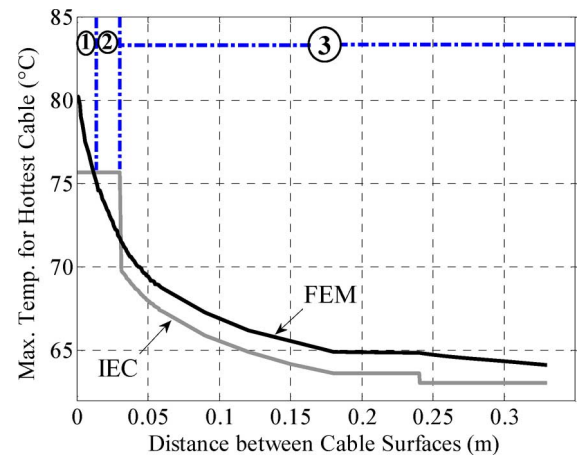


Fig. 8. Steady-state temperature for the center conductor in the group at 25°C ambient temperature and 60-W/m power loss in each cable. The cable construction is given in Fig. 18(a).

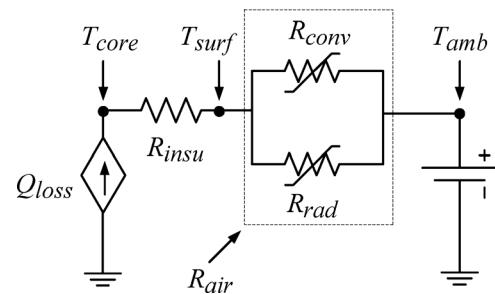


Fig. 9. Thermal–electrical equivalent circuit for a single-core cable.

has been considered unity ( $\varepsilon = 1$ ) to produce a fair comparison with the IEC method. The results are given in Fig. 4. As one can see, the difference between the simulation results and the IEC is noticeable (up to 12%). From the simulation, it has been observed that the hottest cable in the group is always the cable

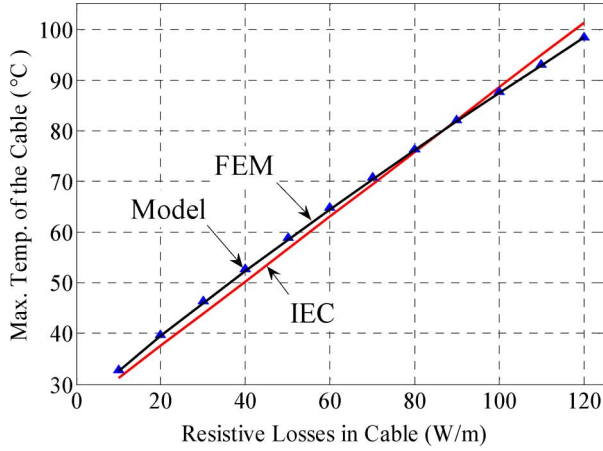


Fig. 10. Comparison of steady-state conductor temperature obtained for a single-core cable with the model of Fig. 9, and FEM at 25°C ambient temperature. The cable construction is given in Fig. 18(a).

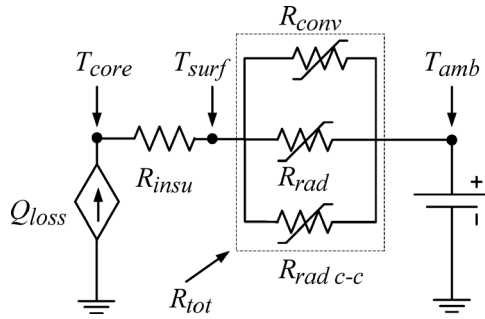


Fig. 11. Thermal-electrical equivalent circuit for one of the three cables in a horizontal group.

on top, while the IEC assumes that all three cables have the same temperature.

**D. Group of Horizontal Cables (Touching and Not Touching)**

Another one of the most commonly used installation methods for cables, especially in three-phase systems, is three horizontal cables touching and separated as shown in Fig. 5. Heat-transfer FEM simulations have been performed by assuming that the cables are equally loaded. Also, to make the simulation conditions closer to the IEC standard, it is assumed that cables have black body surfaces ( $\epsilon = 1$ ). Finite-element and IEC-based calculation results for the hottest cable as a function of distance between cables are shown in Fig. 6. This figure can be analyzed in three distinct regions:

- Region 1) When cables are touching or are very close to each other (maximum separation of around  $0.1 D_c^*$ ).
- Region 2) When cables are separated from each other, but the separation distance is not sufficient for the cables to be isolated from each other.
- Region 3) When cables are sufficiently far from each other and induced heating is negligible.

Grouping cables affect the heat transfer because of proximity effects (induced heating). Whenever cables are touching, grouping plays a dominant role since contact prevents cables from transferring heat to the surrounding air. This behavior can be observed in Fig. 5 (Region 1). In this region, the final

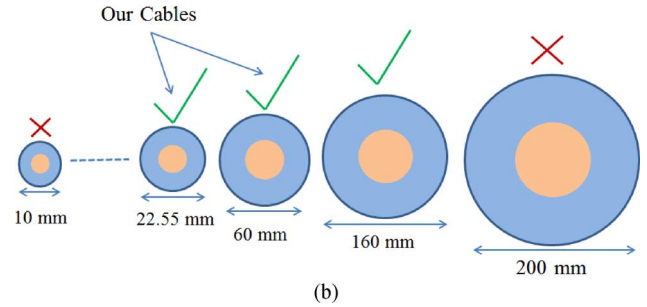
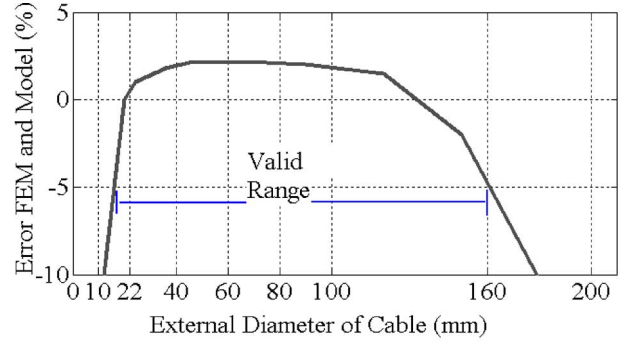


Fig. 12. Results of an exhaustive parametric analysis. (a) Validity range of (13) according to the error with respect to FEM and (b) validity range of (13) based on changing the external diameter of the cable.

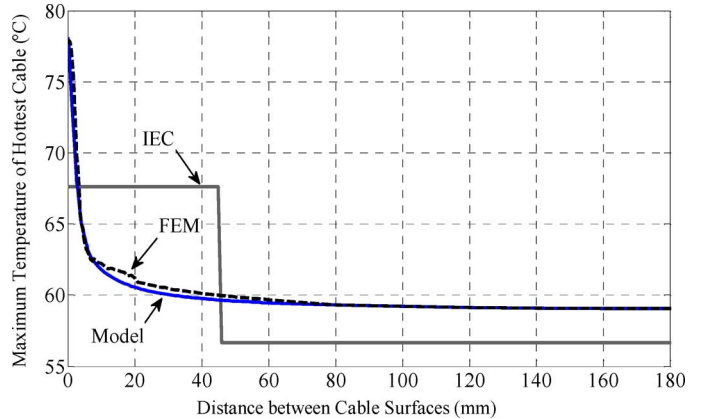


Fig. 13. Comparison of the steady-state temperature obtained for the hottest cable in a horizontal grouping between the model (13), IEC and FEM at 25°C ambient temperature and 50-W/m power losses in the cables. The cable construction is given in Fig. 18(a).

calculated temperature with the IEC equations is substantially lower than the results from FEM simulations. This is so because in the IEC, the proximity effects are not modeled in a proper manner. In Region 2, cables are separated from each other and convection heat transfer takes place. The IEC in this region assumes that cables are touching, which is obviously incorrect. Therefore, the final temperature for the hottest cable is lower in reality than the calculated temperature with the IEC formulas. In Region 3, the IEC considers that the proximity effect is negligible and each cable can be assumed to be isolated. This is correct; however, based on the observation of the FEM simulations shown in Fig. 6, one can see a difference of about 2 °C between FEM and IEC. This result is coherent with the case of one isolated cable given in Section II and shown in Fig. 10.

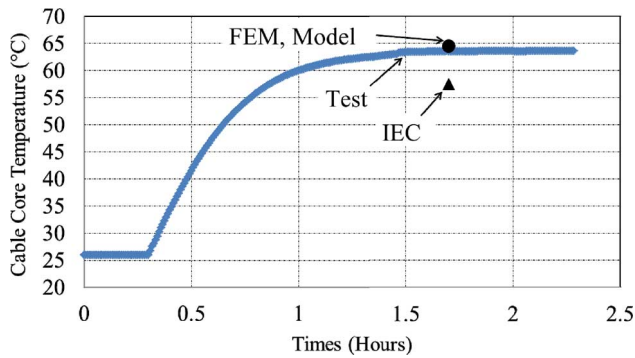


Fig. 14. Comparison of the laboratory experiment, FEM, proposed model (13), and IEC results for the center cable of a touching horizontal formation at 26 °C ambient temperature and carrying 350 A. The cable construction is given in Fig. 18(b).

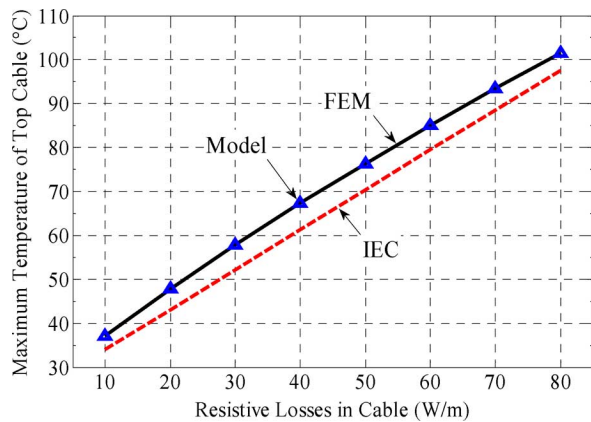


Fig. 15. Comparison of the steady-state temperature obtained for the top cable in trefoil formation by model IEC and FEM at 25 °C ambient temperature. The cable construction is given in Fig. 18(a).

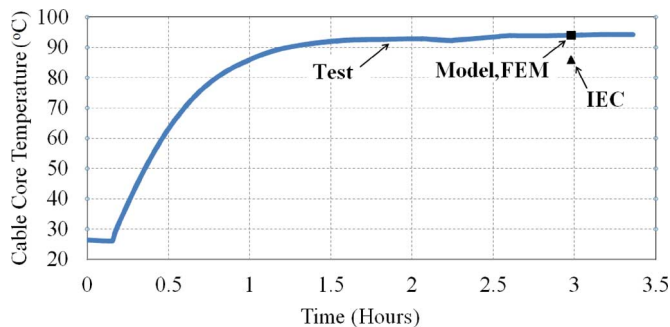


Fig. 16. Laboratory experiment, FEM, model of Fig. 11, and IEC results for the top cable of the trefoil formation at 26 °C ambient temperature and carrying 450 A. The cable construction is given in Fig. 18(b).

This point corresponds to the case of for 50-W/m losses in the cable. Note that for a different case, the differences between FEM and IEC can be larger (up to 5 °C).

#### E. Group of Vertical Cables (Touching and Not Touching)

Another common installation method for grouped cables is the vertical arrangement. Three equally loaded cables in vertical position have been simulated as shown in Fig. 7. Finite element and IEC calculated temperature for the hottest cable as

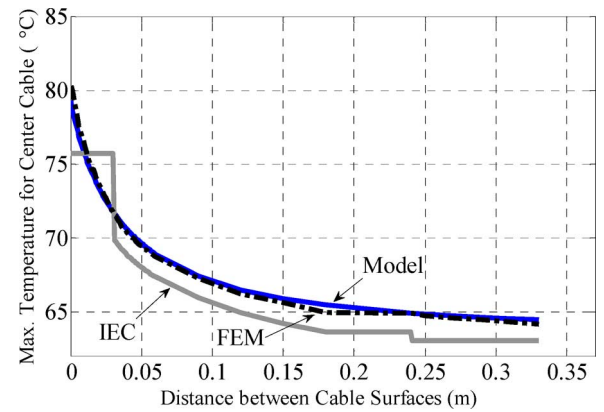


Fig. 17. Comparison of the steady-state temperature obtained for the center cable in a vertical group by model IEC and FEM at 25 °C ambient temperature and 60-W/m power losses in the cables. The cable construction is given in Fig. 18(a).

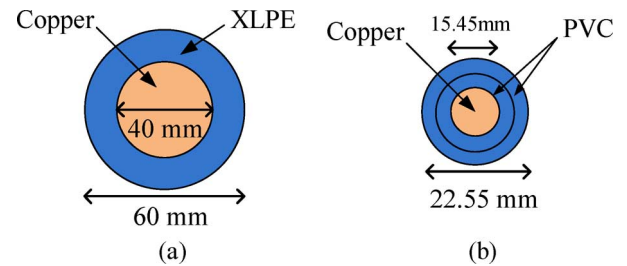


Fig. 18. Specification of the cables: (a) cable used for general FEM simulations and (b) cable used in experiments.

a function of distance between cables are presented in Fig. 8. Note that the emissivity for the cable surfaces has been assumed equal to 1.0 (black body). The results show that there are many similarities with the case with cables installed in the horizontal configuration. The most important difference is that in the vertical configuration, heat convection from the cables below contributes more to the proximity effect. In fact, because the cables are placed one on top of the other, the heat dissipated from the lower cables increases the temperature of the cables above. When the cables are touching, or very close to each other, the hottest cable is the one in the center of the group. When the separation distance increases, the hottest spot migrates to the cable on top, while in the horizontal grouping, the center cable is always the hottest. As before, there are three distinguishable regions for the thermal behavior of vertically separated groups of cables:

- Region 1) When cables are touching or are very close to each other.
- Region 2) When cables are at a distance from each other, but the proximity effect is not negligible.
- Region 3) When cables are far from each other and proximity effects are negligible.

When cables are separated from each other around a distance of 4 times the diameter of the cable  $D_e^*$ , the proximity effect is negligible. Notice that in the vertical configuration, cables should be separated more than in the horizontal formation to be considered as isolated cables. This fact is observable in Fig. 8 where the separation distance ( $x$ -axis) is in meters rather than

in millimeters. In Region 1, the IEC does not consider the proximity effect accurately; therefore, the computed temperature for the hottest cable is lower than in reality. The IEC underestimates the temperature in the same fashion as for horizontal cables. Discussion and reasons for the thermal behavior of horizontally installed cables apply for regions 2 and 3 and, thus, they are not repeated.

### III. THERMAL-ELECTRICAL EQUIVALENT CIRCUIT

In this section, a physical equivalent thermal circuit that considers the missing parameters in the IEC Standards is proposed. The validity of the model has been tested with finite-element simulations and laboratory experiments. The thermal circuit consists of four individual elements:

- 1)  $Q_{\text{loss}}$ : Current source which represents the heat losses in the cable. These losses are temperature dependent and computed per IEC Standard 60287-1-1.
- 2)  $R_{\text{insu}}$ : Thermal resistance of the cable insulation, which is calculated per [1]. The model is compatible with other cable constructions by substituting the proper ladder-type equivalent circuit. For our cable, we have

$$R_{\text{insu}} = \frac{\rho_t}{2\pi} \ln \left[ 1 + \frac{2t_1}{d_c} \right] \quad (5)$$

where

- $\rho_t$  thermal resistivity of insulation (k.m/W);
- $t_1$  thickness of insulation (in meters);
- $d_c$  conductor diameter of the cable (in meters).

- 3)  $R_{\text{air}}$  is the thermal resistance of the surrounding air. This nonlinear resistance is obtained from the parallel equivalent of the radiation and natural convection resistances. Note that the resulting equivalent thermal resistance is nonlinear because the heat-transfer coefficients vary with the temperature of the cable surface. The resistances can be computed as in [4]

$$R_{\text{conv}} = \frac{1}{h_{\text{conv}} S} \quad (6)$$

$$R_{\text{rad}} = \frac{1}{h_{\text{rad}} S} \quad (7)$$

$$R_{\text{air}} = R_{\text{conv}} \parallel R_{\text{rad}} \quad (8)$$

where  $S$  is the total area exposed ( $\text{m}^2$ );  $h_{\text{conv}}$  and  $h_{\text{rad}}$  are the heat-transfer coefficients for convection and radiation and are obtained from (3) and (4). For the calculation of  $h_{\text{conv}}$ , one needs to know the Nusselt and Rayleigh numbers ( $Nu$ ,  $Ra_D$ ) which can be obtained from [4]

$$Nu = \left[ 0.6 + \frac{0.387 Ra_D^{1/6}}{\left[ 1 + \left( \frac{0.559}{Pr} \right)^{9/16} \right]^{8/27}} \right]^2 \quad (9)$$

$$Ra_D = \frac{g P_r \beta D_e^* (T_s - T_{\text{amb}})}{v^2} \quad (10)$$

where  $P_r$  is Prandtl number for air, which varies with air temperature and can be obtained from tables of physical properties [4],  $\beta$  is the volumetric thermal expansion of air in ambient temperature ( $\text{K}^{-1}$ ),  $g$  is the gravity acceleration ( $\text{m/s}^2$ ), and  $v$  ( $\text{m}^2/\text{s}$ ) is kinematic viscosity of the air at ambient temperature.

- 4) A voltage source that represents the ambient temperature. This equivalent circuit is shown in Fig. 9.

Since the thermal resistances  $R_{\text{air}}$ ,  $R_{\text{conv}}$ , and  $R_{\text{rad}}$  are nonlinear, one applies an iterative algorithm to compute the steady-state temperature of the cable when using the equivalent circuit of Fig. 9. The comparison of the attained temperature computed with finite elements and the proposed model is given in Fig. 10. The results show a perfect match between the model of this paper and FEM simulations. It is a physical fact that the cable surface is not an isothermal. The hottest point on the surface of the cable is at the top, and the point at the bottom of the cable has the lowest temperature. Empirical correlations have been used to compute  $R_{\text{conv}}$  and, consequently,  $R_{\text{air}}$ . These specific equations allow for  $R_{\text{air}}$  to be calculated using the temperature of the cable at the point in the middle. Our model, however, is able to calculate the precise value for the conductor temperature, which is the factor that determines the ampacity.

#### A. Thermal Circuit for the Group of Horizontal Cables

1) *Touching and Close Distance Up to  $0.1 D_e^*$* : When a group of horizontal cables is touching or very close to each other (under  $0.1 D_e^*$ ), convection from the surface of the cable is restricted, especially for the center cable. Radiation from cable surfaces to each other also depends on the position of the cable in the group. Based on its position, each cable in the group has a unique heat dissipation coefficient. A general thermal circuit applicable to each cable is introduced in Fig. 11.

Note that all nonlinear resistances vary for each cable according to their unique heat dissipation coefficients. The most challenging part in the circuit of Fig. 11 is to obtain the total external resistance ( $R_{\text{tot}}$ ) of each cable.  $R_{\text{tot}}$  is the parallel combination of the convection resistance to air ( $R_{\text{conv}}$ ), radiation resistance to air ( $R_{\text{rad}}$ ), and mutual radiation resistance to the other cables ( $R_{\text{radc-c}}$ ). Radiation from cables to each other depends on the portion of the cable surface which faces the other cables. This parameter can be represented with the view factor, which can be obtained from [4] as

$$F_{c-c} = \frac{1}{\pi} \left[ (X^2 - 1)^{1/2} + \frac{\pi}{2} - \cos^{-1} \frac{1}{X} - X \right] \quad (11)$$

$$X = 1 + \frac{D_{\text{is}}}{D_e^*} \quad (12)$$

where  $D_{\text{is}}$  is the distance between cable surfaces (in meters).

As stated before, each cable in the group has unique physics which creates a unique heat coefficient for the cable. However, in ampacity calculations, the hottest cable in the group determines the ampacity of the circuit. The following equation is

proposed in this paper for the calculation of the total heat dissipation coefficient ( $h_{tot}$ ) for the center cable

$$h_{tot} = h_1 \times \left( \frac{D_e^{*1.7} - D_{is}^{1.7}}{D_e^{*1.7}} \right)^{D_{is}/D_e^*} + h_2 \times \left( \frac{D_{is}}{D_e^*} \right)^{1.4} \quad (13)$$

where from [4], [7], and [11], one obtains

$$h_1 = \frac{0.7011}{\pi \alpha_c (D_e^*)^{0.25}} + \left( \frac{\varepsilon \alpha_r}{\pi \alpha_c} \right) (1 - 0.364\varepsilon) \quad (14)$$

$$h_2 = \frac{0.7k_{amb}}{D_e^* (T_s - T_{amb})^{0.25}} + \frac{1}{\pi \alpha_c (T_s - T_{amb})^{0.25}} + \left( \frac{\varepsilon \alpha_r}{\pi \alpha_c} \right) (1 - 2F_{c-c}\varepsilon) \quad (15)$$

with

$$\alpha_r = \frac{\sigma}{0.42k_{amb}(T_s - T_{amb})} \cdot \left[ \frac{v^2}{\beta g p_r (T_s - T_{amb})} \right]^{0.25} (T_s^4 - T_{amb}^4) \quad (16)$$

$$\alpha_c = \frac{1}{0.42\pi k_{amb}} \left[ \frac{v^2}{\beta g p_r} \right]^{0.25} \quad (17)$$

Equation (14) represents the heat dissipation coefficient for the center cable in the group when cables are touching and (15) is the heat dissipation coefficient for the center cable when cables are separated from each other by more than  $0.1 D_e^*$ .

Both (14) and (15) are empirical expressions which can be combined together and provide a more precise and realistic value for the heat dissipation coefficient for all regions (1–3). From the observation of numerous FEM simulations and mathematical fitting, (14) and (15) are combined into (13) to give a unified formulation for all three regions. Fig. 12 shows the results of an exhaustive parametric study aimed to determine the validity range of the model. Note that (13) is valid when the outer diameter of the cable varies in the range from 15 to 160 mm, which covers most power cables. The difference between the model and FEM simulations in this range is less than 5%. The total external resistance for the center and side cables can be obtained from [4] and [7]:

$$R_{tot} = \frac{1}{\pi D_e^* (T_s - T_{amb})^{0.25} h_{tot}} \quad (18)$$

A comparison of the steady-state conductor temperature for the center cable between the IEC method, finite elements, and the model is given in Fig. 13. The results show a very good match between the model and FEM simulations. Note that radiation to the other cables has been calculated as a portion of radiation to the ambient by considering the view factor. When the cables are thermally coupled, the dominant factor for heat dissipation is convection.

A laboratory experiment consisting of three sections of the cable presented in Fig. 18(b) (see the Appendix) has been set up in a horizontal touching formation. The current in all three cables was fixed at 350 A during the test. The temperature of the center cable in the group (the hottest cable) was captured

until the steady-state condition was reached. The results from the test, FEM, proposed model, and IEC are shown in Fig. 14. The results of FEM and the model are close to the test, while the IEC method underestimates the steady-state temperature.

2) *Cables Separated by More Than  $0.1 D_e^*$  (Regions 2 and 3 in Fig. 5):* Power cables affect each other when the separation distance exceeds  $0.1 D_e^*$  but is smaller than  $0.75 D_e^*$  (Region 2). For larger separation distances over  $0.75 D_e^*$  (Region 3), they can be treated as isolated cables, and the proximity effects are negligible. The same thermal circuit proposed in Fig. 11 can be applied for these two regions. The total heat dissipation coefficient for the center cable can be derived as follows [7]:

$$h_{tot} = \frac{0.7k_{amb}}{D_e^* (T_s - T_{amb})^{0.25}} + \frac{1}{\pi \alpha_c (T_s - T_{amb})^{0.25}} + \left( \frac{\varepsilon \alpha_r}{\pi \alpha_c} \right) (1 - 2F_{c-c}\varepsilon). \quad (19)$$

Equation (19) is also valid for Region 3, where the cables are far from each other so they can behave as isolated cables. Remember that  $F_{c-c}$  tends to zero when the distance between the cables is large. A comparison between IEC, FEM, and the proposed circuit for the center cable in the group is shown in Fig. 13; one can see a very good match. Note that all cable surfaces have been modeled as a black body (emissivity is 1.0).

### B. Thermal Circuit for Trefoil Formation (Touching)

In this cable arrangement, a substantial proximity effect can be observed between cables. The thermal electric circuit of Fig. 11 can be used for the calculation of steady-state temperature of each cable in this formation. Remember that the main interest is on the top cable (hottest cable). The total heat dissipation coefficient for the top cable is [7]

$$h_{tot} = \frac{0.402}{1.188\pi \alpha_c (D_e^*)^{0.25}} + \left( \frac{\varepsilon \alpha_r}{\pi \alpha_c} \right) (0.833 - 0.182\varepsilon). \quad (20)$$

By substituting the heat dissipation coefficient (20) into (18), one can obtain the total external resistance for the top cable in the trefoil formation and calculate the final steady-state temperature of the cable. The steady-state temperature of the top cable as a function of the resistive losses in the cable has been computed with the proposed model. All cables in trefoil formation are equally loaded and are identical. In all cases, a black body surface is assumed ( $\varepsilon = 1$ ). The steady-state temperature of the top cable, computed with the proposed model and compared with FEM and IEC, is shown in Fig. 15. Results from the model of this paper perfectly match FEM while IEC underestimates the attained temperature.

In addition to FEM simulations, a laboratory experiment has been performed on a trefoil formation. Three sections of the cable depicted in Fig. 18(b) have been set up in a trefoil formation. The current in all three cables was fixed at 450 A during the test. The temperature of the top cable in the group (the hottest cable) was captured until the steady-state condition was reached. The conductor of the cable is made of copper with a diameter of 15.45 mm; the insulation is PVC with an external diameter of 22.55 mm, and the surface emissivity of the cable is 0.87 (according to manufacturer data). Thermocouples have

been used to capture the conductor of the cable temperature continuously at different points along the top cable of the trefoil formation. The results from the test, FEM simulation, proposed model, and IEC method are shown in Fig. 16. As can be seen, the results from the test, FEM, and model match each other, while the IEC method underestimates the temperature of the conductor at steady state.

### C. Thermal Circuit for Group Vertical Cables (Touching and Not Touching)

As mentioned before for this particular installation type, heat convection from the lower cables affects the upper cables in the group. Radiation of the cables to each other remains the same as the radiation of the cables in the horizontal grouping since they are facing each other in the same fashion and, thus, the view factor does not change. The equivalent thermal circuit for this configuration is the same as the one in Fig. 11. Notice that as before, each cable in the group has its own unique heat dissipation coefficient. Therefore, for the calculation of the final temperature of each cable, one should substitute the different total nonlinear external resistances in the circuit. Here, the heat dissipation coefficient for the center cable is introduced because it is almost always the hottest cable in the group and determines the ampacity. When the cable in the center is not the hottest, its temperature is very close to the maximum. The following equation gives the total heat dissipation coefficient ( $h_{tot}$ ) for the center cable [7]:

$$h_{tot} = \frac{0.7k_{amb} + \frac{D_e^{*0.75}(T_s - T_{amb})^{0.25}}{\pi\alpha_c}}{D_e^*(T_s - T_{amb})^{0.25} + D_e^{*0.25}\Omega \left(0.7\pi\alpha_c + D_e^{*0.75}(T_s - T_{amb})^{0.25}\right)} + \left(\frac{\varepsilon\alpha_r}{\pi\alpha_c}\right)(1 - 2F_{c-c}\varepsilon) \quad (21)$$

where

$$\Omega = 1.18 \left( \frac{D_e^*}{2(D_e^* + D_{is})} \right)^{1.75} \quad (22)$$

$\Omega$  in (22) is the contribution factor to the center cable from the other cables in the group. When cables are close to each other (for  $D_{is} = 0$  up to 4 times  $D_e^*$ ),  $\Omega$  has more contribution to the heat dissipation coefficient and for larger separation distances (for  $D_{is}$  more than 4 times  $D_e^*$ ),  $\Omega$  tends to zero. The total external resistance of the center cable can be obtained from (18). Results for the FEM simulation, the proposed model, and the IEC method are shown in Fig. 17.

## IV. CONCLUSION

Computation of the steady-state temperature of power cables in free air for the most common configurations has been investigated. It has been shown that the IEC standard calculation methods produce optimistic results when not used within their scope. This paper has presented improvements to the IEC standards to rate cables under general operating conditions. Accurate thermal-electrical equivalent circuits have been proposed

for the different cable geometric configurations in air. The proposed models properly consider all physical parameters, such as emissivity and adequate heat dissipation coefficients for convection and radiation per cable. The validity of the models has been established with numerous FEM simulations and experimental tests.

## APPENDIX

The construction information of the two cables used in this paper is given in Fig. 18. Fig. 18(a) describes the cable used for most of the FEM simulations, while Fig. 18(b) describes the cable that was tested in the laboratory.

A set of links to download the COMSOL files to reproduce the FEM simulations of this paper can be found at <http://power.poly.edu/images/stories/data.pdf>

## ACKNOWLEDGMENT

The authors would like to thank the reviewers for their valuable comments. Their comments proved to be of great guidance to enhance this work.

## REFERENCES

- [1] IEC Standard-Electric Cables – Calculation of the Current Rating – Part 2: Thermal Resistance – Section 1: Calculation of the Thermal Resistance, IEC Standard 60287-2-1, 1994–12.
- [2] V. T. Morgan, “Effect of surface-temperature rise on external thermal resistance of single-core and multi-core bundled cables in still air,” in *Proc. IEEE Gen. Transm. Distrib.*, May 1994, vol. 141, pp. 215–218.
- [3] G. Anders, *Rating of Electric Power Cables: Ampacity Computations for Transmission, Distribution, and Industrial Applications*. New York: IEEE, 1997.
- [4] F. P. Incropera, *Introduction to Heat Transfer*. New York: Wiley, 1996, p. 465.
- [5] Reviewer 1, Comments to the Authors of First Revision of paper TPWRD-00953-2013.
- [6] S. Whitehead and E. E. Hutchings, “Current rating of cables for transmission and distribution,” *J. Inst. Elect. Eng.*, vol. 83, pp. 517–557, Oct. 1938.
- [7] P. Slaninka, “External thermal resistance of air-installed power cables,” *Proc. Inst. Elect. Eng.*, vol. 116, pp. 1547–1552, 1969.
- [8] V. T. Morgan, “External thermal resistance of aerial bundled cables,” in *Proc. IEEE Gen. Transm. Distrib.*, Mar. 1993, vol. 140, pp. 65–72.
- [9] M. Terracciano, S. Purushothaman, F. de León, and A. V. Farahani, “Thermal analysis of cables in unfilled troughs: Investigation of the IEC standard and a methodical approach for cable rating,” *IEEE Trans. Power. Del.*, vol. 27, no. 3, pp. 1423–1431, Jul. 2012.
- [10] “Comsol Multiphysics,” Comsol AB Group, 2006, Heat Transfer Module User’s Guide.
- [11] G. F. Marsters, “Arrays of heated horizontal cylinders in natural convections,” in *Int. J. Heat Mass Transfer*. New York: Pergamon, 1972, vol. 15, pp. 921–933.



**Ali Sedaghat** (S’13) was born in Kermanshah, Iran, in 1978. He received the B.Sc. degree in electrical power engineering from the Iran University of Science and Technology (IUST), Tehran, Iran, in 2001 and is currently pursuing the Ph.D. degree in electrical engineering at the NYU Polytechnic School of Engineering, Brooklyn, NY, USA.

His research interests include the thermal analysis of power cables in air, application of flexible ac transmission systems devices in power systems, and re-configuration of distribution systems.





**Francisco de León** (S'86–M'92–SM'02) received the B.Sc. and M.Sc. (Hons.) degrees in electrical engineering from the National Polytechnic Institute, Mexico City, Mexico, in 1983 and 1986, respectively, and the Ph.D. degree in electrical engineering from the University of Toronto, Toronto, ON, Canada, in 1992.

He has held several academic positions in Mexico and has worked for the Canadian electric industry. Currently, he is an Associate Professor at NYU Polytechnic School of Engineering, Brooklyn, NY, USA.

His research interests include the analysis of power phenomena under nonsinusoidal conditions, the transient and steady-state analyses of power systems, the thermal rating of cables and transformers, and the calculation of electromagnetic fields applied to machine design and modeling.